

# INCREASING AND DECREASING SEQUENCES IN FILLINGS OF MOON POLYOMINOES

MARTIN RUBEY

**ABSTRACT.** We present an adaptation of *jeu de taquin* for arbitrary fillings of moon polyominoes. Using this construction we show various symmetry properties of such fillings taking into account the lengths of longest increasing and decreasing chains. In particular, we prove a conjecture of Jakob Jonsson. We also relate our construction to the one recently employed by Christian Krattenthaler, thus generalising his results.

## 1. INTRODUCTION

Recently, a great variety of authors became interested in symmetry properties of the number of fillings of certain shapes taking into account the lengths of the longest increasing and decreasing chains. This topic comes about also in a different guise, namely in terms of crossings and nestings of partitions. Some recent papers are [5, 9, 10, 11, 12].

Our main goal is to confirm Jakob Jonsson's Conjecture [9], which is Theorem 5.2 of this article. The proof is surprisingly simple, especially taking into account the complicated arguments originally needed to prove a special case.

Although not completely bijective, the key construction is an adaptation of *jeu de taquin* to so-called moon polyominoes, see Definition 2.2. Similar to *jeu de taquin* it turns out that the order of carrying out the basic operations of our construction is irrelevant.

Apart from proving the above mentioned conjecture we relate the bijection used in this article to the one used by Christian Krattenthaler in [12].

We would also like to mention the series of papers [1, 2, 13] studying non-crossing and non-nesting partitions in Coxeter groups. In a forthcoming article we will show that the bijection presented here can be modified to work for the setting described in these papers.

## 2. DEFINITIONS

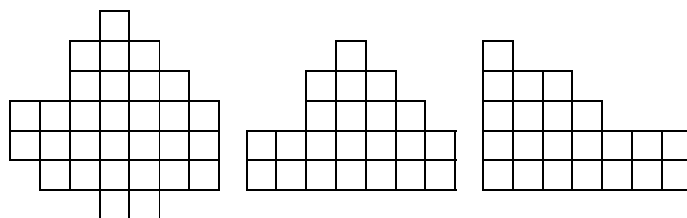
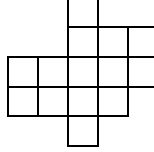


FIGURE 1. a moon-polyomino, a stack-polyomino and a Ferrers diagram

**Definition 2.1.** A *polyomino* is a finite subset of  $\mathbb{Z}^2$ , where we regard an element of  $\mathbb{Z}^2$  as a box. A *column* of a polyomino is the set of boxes along a vertical line. The polyomino is *column- and row-convex* if for any two boxes in a column, the elements of  $\mathbb{Z}^2$  in-between are also boxes of the polyomino, and for any two boxes in a row, the elements of  $\mathbb{Z}^2$  in-between are also boxes of the polyomino. It is *intersection-free*, if any two columns are *comparable*, i.e., one of them both begins at a higher level and ends at a lower one.

For example, the polyomino



is row- and column-convex, but not intersection free, since the first and the last columns are incomparable.

**Definition 2.2.** A *moon polyomino* is a column-convex, intersection-free polyomino. A *stack polyomino* is a moon-polyomino if all columns start at the same level. A *Ferrers diagram* is a stack-polyomino with weakly increasing row widths  $\lambda_1, \lambda_2, \dots, \lambda_n$ , reading rows from bottom to top.

*Remark.* We alert the reader that we are using ‘French’ notation for Ferrers diagrams.

In the following we will consider ‘fillings’ of such polyominoes with natural numbers, satisfying various conditions.

**Definition 2.3.** An arbitrary *filling* of a polyomino is an assignment of natural numbers to the boxes of the polyomino. In a *0-1-filling* we restrict ourselves to the numbers 0 and 1. A *standard filling* has the additional constraint that in each column and in each row there is exactly one entry 1, whereas a *partial filling* has at most one entry 1 in each column and in each row.

In the figures, we will usually omit zeros, and in 0-1-fillings we will replace ones by crosses for aesthetic reasons. For other fillings, we will refer to the number in a box usually as the *multiplicity* of an entry.

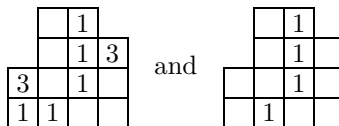
In this article we are mainly interested in the lengths of certain chains in such fillings.

**Definition 2.4.** A *north-east chain*, or short *ne-chain* of length  $k$  in an arbitrary filling of a moon polyomino is a sequence of  $k$  non-zero entries, such that each entry is strictly to the right and strictly above the preceding entry in the sequence. Furthermore, we require that the smallest rectangle containing all entries of the sequence is completely contained in the moon polyomino. Similarly, in a *south-east chain*, for short *se-chain*, each entry is strictly to the right and strictly below the preceding entry.

*NE-chains* and *SE-chains* may have entries in the same column and in the same row. For these kinds of chains, each entry contributes its size to the length of a sequence, i.e., a *NE-chain* of length  $k$  is a sequence of entries, such that each entry is weakly to the right and weakly above the preceding entry in the sequence, and the sum of the entries equals  $k$ .

For 0-1-fillings we also define *nE-chains* and *sE-chains*, where we allow an entry of the sequence to be in the same column as its predecessor, but not in the same row. Similarly, entries of *Ne-chains* and *Se-chains* are allowed to be in the same row, but not in the same column.

For example, consider the following two fillings:



The length of the longest ne-chain in the filling on the left is three, whereas the length of the longest se-chain is two. The lengths of the longest NE- and SE-chains are six and five respectively.

The lengths of the longest nE-, Ne-, sE-, and Se-chains in the 0-1-filling on the right are four, two, three and one respectively.

Finally, we need the notions of partition and semi-standard Young tableau:

**Definition 2.5.** A *partition* is a weakly decreasing sequence of natural numbers, which are called its *parts*. The *length* of a partition is the number of its parts, the *size* of a partition is the sum of its parts. A partition  $\lambda = (\lambda_1, \lambda_2, \dots, \lambda_l)$  is *contained* in another partition  $\mu = (\mu_1, \mu_2, \dots, \mu_m)$  if  $l \leq m$  and  $\lambda_i \leq \mu_i$  for all  $i \leq l$ .

The union of  $\lambda$  and  $\mu$ , denoted  $\lambda \cup \mu$ , is the partition  $\kappa = (\kappa_1, \kappa_2, \dots, \kappa_k)$  with  $k = \max(l, m)$  and  $\kappa_i = \max(\lambda_i, \mu_i)$  for all  $i \leq k$ , where we set  $\lambda_i = 0$  for  $i > l$  and  $\mu_i = 0$  for  $i > m$ .

The *transpose* or *conjugate* of a partition  $\lambda$  is defined as  $\lambda^t = (\mu_1, \mu_2, \dots, \mu_m)$ , where  $m = \lambda_1$  and  $\mu_i$  is the number of parts in  $\lambda$  greater than or equal to  $i$ .

The *transpose* of a sequence of partitions  $P = (\emptyset = \lambda^0, \lambda^1, \dots, \lambda^n)$  is the sequence of partitions  $P^t$  obtained by transposing each individual partition.

*Remark.* We remind the reader that each Ferrers shape (in French notation) corresponds to a partition  $\lambda$ , setting  $\lambda_i$  to the length of the  $i^{\text{th}}$  row from bottom to top. Using this correspondence, the transpose of a partition can be obtained by reflecting the corresponding Ferrers shape about the main diagonal.

**Definition 2.6.** A *semi-standard Young tableau* is a filling of a Ferrers shape with positive integers, such that entries are weakly increasing in rows and strictly increasing – from bottom to top – in columns.

A *standard Young tableau* is a semi-standard Young tableau with entries being the numbers 1 through  $n$ , such that each number occurs exactly once.

A *partial Young tableaux* is a semi-standard Young tableaux with all entries distinct.

An example for a pair of standard Young tableaux is given in Equation (1).

### 3. GROWTH DIAGRAMS AND THE ROBINSON-SCHENSTED-KNUTH CORRESPONDENCE

Sergey Fomin's growth diagrams together with Marcel Schützenberger's *jeu de taquin* [8, 14, 15] will be the central tools in this article. Although the contents of this section is well known, we reproduce it here for the convenience of the reader. Some additional information and more references can be found in [12, Sections 2 and 4].

**3.1. Local Rules.** Consider a rectangular polyomino with a partial filling, as, for example, in Figure 3.a where we have replaced zeros by empty boxes and ones by crosses. Using the following construction we will inductively label the corners of each box with a partition, starting from the bottom left corner.

First, we attach the empty partition  $\emptyset$  to the corners along the lower and the left border. Suppose now that we have already labelled all the corners of a square

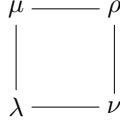


FIGURE 2. a cell of a growth diagram

except the top right with partitions  $\lambda$ ,  $\mu$  and  $\nu$ , as in Figure 2. We compute  $\rho$  as follows:

- F1 Suppose that the square does not contain a cross, and that  $\lambda = \mu = \nu$ . Then set  $\rho = \lambda$ .
- F2 Suppose that the square does not contain a cross, and that  $\mu \neq \nu$ . Then set  $\rho = \mu \cup \nu$ .
- F3 Suppose that the square does not contain a cross, and that  $\lambda \subset \mu = \nu$ . Then we obtain  $\rho$  from  $\mu$  by adding 1 to the  $i + 1^{\text{st}}$  part of  $\mu$ , given that  $\lambda$  and  $\mu$  differ in the  $i^{\text{th}}$  part.
- F4 Suppose that the square contains a cross. This implies that  $\lambda = \mu = \nu$  and we obtain  $\rho$  from  $\lambda$  by adding 1 to the first part of  $\lambda$ .

The important fact is, that this process is invertible: given the labels of the corners along the upper and right border of the diagram, we can reconstruct the complete growth diagram as well as the entries of the squares. To this end, suppose that we have already labelled all the corners of a square except the bottom left with partitions  $\mu$  and  $\nu$  and  $\rho$ , as in Figure 2. We compute  $\lambda$  and the entry of the square as follows:

- B1 If  $\mu = \nu = \rho$  we set  $\lambda = \rho$  and leave the square empty.
- B2 If  $\mu \neq \nu$  we set  $\lambda = \mu \cap \nu$  and leave the square empty.
- B3 If  $\mu = \nu \subset \rho$  and  $\mu$  and  $\rho$  differ in the  $i^{\text{th}}$  part for  $i \geq 2$ , we obtain  $\lambda$  from  $\mu$  by deleting 1 from the  $i - 1^{\text{st}}$  part of  $\mu$  and leave the square empty.
- B4 If  $\mu = \nu \subset \rho$  and  $\mu$  and  $\rho$  differ in the first part we set  $\lambda = \mu$  and mark the square with a cross.

**3.2. The Robinson-Schensted Correspondence and Greene's Theorem.** In the case of a standard filling of a square, the sequence of partitions  $\emptyset = \mu^0, \mu^1, \dots, \mu^n$  along the upper border of the growth diagram corresponds to a standard Young tableau  $Q$  as follows: we put the entry  $i$  into the cell by which  $\mu^{i-1}$  and  $\mu^i$  differ. Similarly, the sequence of partitions  $\emptyset = \lambda^0, \lambda^1, \dots, \lambda^n$  along the right border of the diagram corresponds to a standard Young tableau  $P$  of the same shape as  $Q$ .

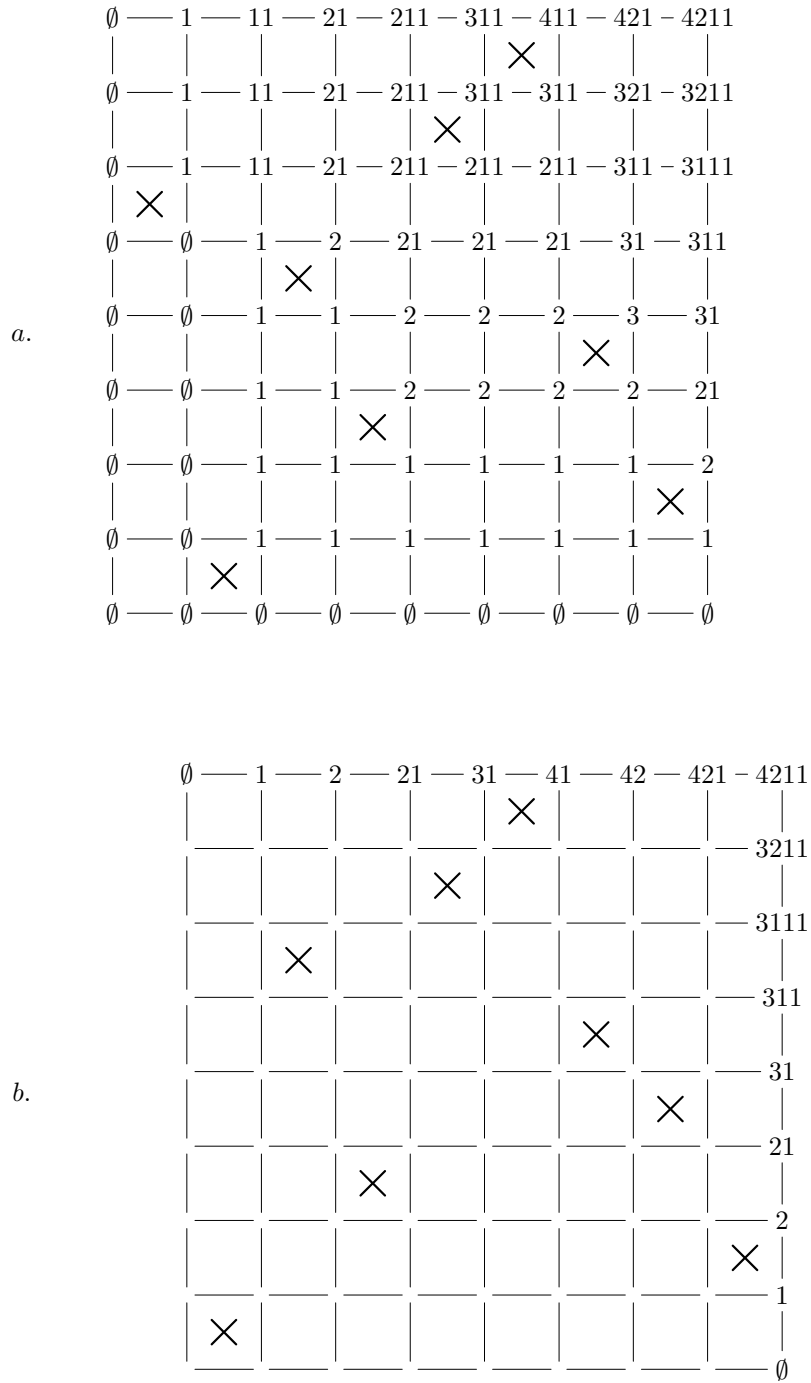
Furthermore, the filling itself defines a permutation  $\pi$ . For example in Figure 3.a we have  $\pi = 6, 1, 5, 3, 7, 8, 4, 2$  and

$$(1) \quad (P, Q) = \left( \begin{array}{|c|c|c|c|} \hline 6 & & & \\ \hline 5 & & & \\ \hline 3 & 7 & & \\ \hline 1 & 2 & 4 & 8 \\ \hline \end{array}, \begin{array}{|c|c|c|c|} \hline 8 & & & \\ \hline 4 & & & \\ \hline 2 & 7 & & \\ \hline 1 & 3 & 5 & 6 \\ \hline \end{array} \right).$$

It is well known that  $Q$  is simply the recording and  $P$  the insertion tableau produced by the Robinson-Schensted correspondence, applied to the permutation  $\pi$ .

Since the partitions along the upper and right border of a growth diagram determine the filling and vice versa, the following definition will be useful:

**Definition 3.1.** Let  $\pi$  be a standard filling of a square polyomino and consider the corresponding growth diagram. Suppose that the corners along the right border


 FIGURE 3. a. a growth diagram b. *jeu de taquin* on the upper border

are labelled with a sequence of partitions  $P$ , and along the upper border with a sequence of partitions  $Q$ . We then say, that  $\pi$  *corresponds* to the pair  $(P, Q)$ .

For our purposes it is of great importance that the partitions appearing in the corners of a growth diagram also have a ‘global’ description. This is called Greene’s Theorem:

**Theorem 3.2.** [15, Theorem A.1.1.1] *Suppose that a corner  $c$  of the growth diagram is labelled by the partition  $\lambda$ . Then, for any integer  $k$ , the maximal cardinality of the union of  $k$  north-east chains situated in the rectangular region to the left and below of  $c$  is equal to  $\lambda_1 + \lambda_2 + \cdots + \lambda_k$ . Similarly, the maximal cardinality of the union of  $k$  south-east chains situated in the rectangular region to the left and below of  $c$  is equal to  $\mu_1 + \mu_2 + \cdots + \mu_k$ , where  $\mu$  is the transpose of  $\lambda$ .*

**3.3. Variations of the Robinson-Schensted Correspondence.** In the following, we extend the construction described in the previous Section to arbitrary fillings of rectangular polyominoes. To begin with, in the case of partial fillings only terminology changes: Instead of a pair of standard Young tableaux  $(P, Q)$  we now obtain a pair of so-called partial Young tableaux, i.e., semi-standard Young tableaux with all entries distinct.

For an arbitrary filling, we construct a new diagram with more rows and columns, and place entries which are originally in the same column or row in different columns and rows in the larger diagrams. A similar strategy is applied to entries larger than one. More precisely, we proceed as follows:

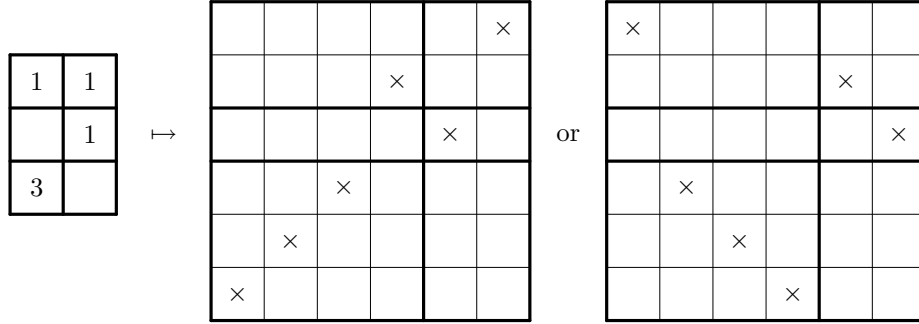


FIGURE 4. Separating entries of an arbitrary filling using RSK or dual RSK'

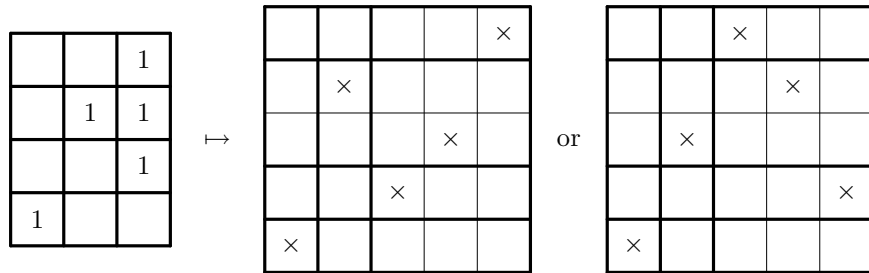


FIGURE 5. Separating entries of a 0-1-filling using dual RSK or RSK'

Each row and each column of the original diagram is replaced with as many rows and columns in the new diagram as it contains entries, counting multiplicities. Then, for each row and for each column of the original diagram we place the entries into the new diagram as a north-east chain. An example can be found in Figure 4, the result being the left of the two blown-up diagrams. Note that this process preserves the length of the NE- and se-chains.

Given a filling  $\pi$  we can apply the rules F1 to F4 to the transformed diagram and obtain a pair of sequences of partitions  $(P, Q)$ . It is well known that the pair

$(P, Q)$  coincides with the result of applying the usual ‘Robinson-Schensted-Knuth’, short RSK correspondence, to  $\pi$ .

There is another obvious possibility to separate the entries of an arbitrary filling. Instead of placing the entries into the new diagram as a north-east chain, we could also arrange them in a south-east chain, thus preserving the length of ne- and SE-chains. An example for this transformation is given in Figure 4, the result being the right of the two blown-up diagrams. In this case, the corresponding sequences of partitions  $(P, Q)$  are the result of the dual RSK’ correspondence, also known as the ‘Burge’ correspondence.

If we restrict ourselves to 0-1-fillings, we can also transform multiple entries of a column of the original diagram into a north-east chain and multiple entries of a row into a south-east chain. We would thus obtain the so-called dual RSK correspondence. In this case, the lengths of nE- and Se-chains are preserved, as can be seen from the example on the left of Figure 5.

As a last possibility, again for 0-1-fillings, we can transform multiple entries of a column of the original diagram into a south-east chain and multiple entries of a row into a north-east chain, obtaining the ‘Robinson-Schensted-Knuth-prime’ correspondence, short RSK’, which preserves the lengths of Ne- and sE-chains. This is shown on the right of Figure 5.

#### 4. VARIATIONS ON JEU DE TAQUIN

Our second tool is *jeu de taquin*, introduced by Marcel Schützenberger, an algorithm that ‘rectifies’ a so-called skew standard Young tableau. For our purposes it is not necessary to introduce skew tableaux, and what we call *jeu de taquin* is sometimes referred to as the  $\Delta$ -operator.

We define *jdt* as an algorithm that takes a partial Young tableau as input and ‘slides out’ the entry 1 of the tableau in the following fashion:

- (1) subtract one from all the entries in the tableau.
- (2) if present, replace the box containing 0 with an empty box. Otherwise stop. In the following, we will move the empty box to the top right border of the tableau.
- (3) if there is no box to the right and no box above the empty box, remove the empty box and stop.
- (4) consider the boxes above and to the right of the box without entry, and exchange the box with the smaller entry and the empty box. Go to Step 3.

*Jeu de taquin* can also be conveniently described with growth diagrams, albeit in a different form than introduced in Section 3.1. Consider a weakly increasing sequence of partitions  $P = (\emptyset = \lambda^0, \lambda^1, \dots, \lambda^n)$  where  $\lambda^{i-1}$  and  $\lambda^i$  differ in size by at most one for  $i \in \{1, 2, \dots, n\}$ . Note that such a sequence corresponds to a partial Young as hinted at at the beginning of Section 3.2. To  $P$  we associate  $\overline{jdt}(P) = (\emptyset = \mu^0, \mu^1, \dots, \mu^n)$ , with the same property as follows:

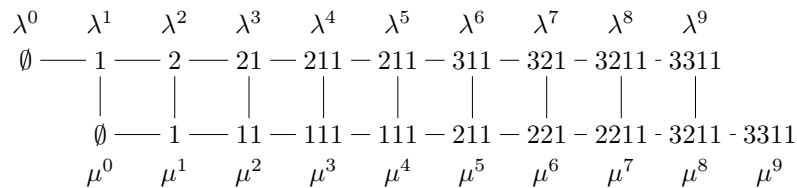


FIGURE 6. Jeu de Taquin

If  $\lambda^1 = \emptyset$ , we set  $\mu^i = \lambda^{i+1}$  for  $i < n$  and  $\mu^n = \lambda^n$ . Otherwise, let  $\mu^0 = \emptyset$ . Suppose that we have already constructed  $\mu^{i-1}$  for some  $i < n$ . Then we distinguish three cases: if  $\lambda^{i+1} = \lambda^i$ , then we set  $\mu^i = \mu^{i-1}$ .

If  $\nu$  is the only partition that contains  $\mu^{i-1}$  and is contained in  $\lambda^{i+1}$ , we set  $\mu^i = \nu$ . Otherwise, there will be exactly one such partition different from  $\lambda^i$ , and we set  $\mu^i$  equal to this partition. Finally, we set  $\mu^n = \lambda^n$ .

An example for this algorithm can be found in Figure 6. Note that, obviously, this algorithm is invertible. To obtain the traditional form of *jeu de taquin*, which we will denote with  $jdt(P)$ , we just need to drop the final partition of  $\overline{jdt}(P)$ .

We can combine growth diagrams as introduced in Section 3.1 and *jeu de taquin* to obtain an interesting bijection on fillings of rectangular polyominoes:

**Definition 4.1.** Let  $\pi$  be a partial filling of a rectangular polyomino and let  $\Delta$  be the associated growth diagram. Let  $j(\Delta)$  be the growth diagram having the same sequence of partitions along the right border as  $\Delta$ , whereas the sequence of partitions along the upper border is obtained by applying  $\overline{jdt}$  to the corresponding sequence of  $\Delta$ . Finally, apply the backward rules B1 to B4 to obtain the remaining partitions and the entries of the squares. Let  $j(\pi)$  be the filling associated to  $j(\Delta)$ .

An example of this transformation can be found in Figure 3. Note that, again, this transformation is invertible.

It turns out that *jeu de taquin* is also intimately connected to the growth diagrams as defined in the previous section. The following proposition is a consequence of [15, Corollary A.1.2.6], as pointed out in the proof of [15, A.1.2.10]:

**Proposition 4.2.** Let  $\pi$  be a partial filling of a rectangular polyomino, and let  $Q$  be the sequence of partitions in the top row of the associated growth diagram. Let  $\omega$  be the filling obtained from  $\pi$  by deleting the first column of the polyomino, and let  $R$  be the sequence of partitions in the top row of the associated growth diagram. Then  $R = jdt(Q)$ .

Before applying this proposition to our situation, we need another definition:

**Definition 4.3.** Two growth diagrams of the same size are *Knuth equivalent* if the partitions labelling the corners along the right border are the same. They are *dual Knuth equivalent* if the partitions labelling the corners along the top border are the same. We use the same terminology for fillings of rectangular polyominoes.

**Corollary 4.4.** Consider the filling  $\pi'$  defined by columns  $i+1, i+2, \dots, i+k$ ,  $i \geq 1$ , of a filling  $\pi$  of a rectangular polyomino. Then  $\pi'$  is dual Knuth equivalent to the filling defined by columns  $i, i+1, \dots, i+k-1$  of  $j(\pi)$ . Furthermore, the filling defined by rows  $i, i+1, \dots, i+k$  of  $\pi$  is Knuth equivalent to the filling defined by the same rows of  $j(\pi)$ .

*Proof.* To obtain the sequence of partitions along the upper border of  $\pi'$ , we only have to delete the first  $i$  columns of the growth diagram and take the first  $k$  partitions labelling the upper border. By Proposition 4.2, this is equivalent to applying  $jdt$   $i$  times to the sequence of partitions along the upper border of  $\pi$  and keeping only the first  $k$  partitions. Obviously, deleting the first column of  $\pi$ , and then the first  $i-1$  columns of the resulting filling is the same as deleting  $i$  columns at once.

To prove the second statement, note first that the sequence of partitions  $P$  along the right border of  $\pi$  and  $j(\pi)$  are the same by definition. To obtain the sequence of partitions of the filling defined by rows  $i, i+1, \dots, i+k$  in  $\pi$  or  $j(\pi)$ , we can apply  $jdt$   $i-1$  times to  $P$  and finally drop all but the first  $k+1$  partitions.  $\square$

In particular, if the entries in columns  $i+1, i+2, \dots, i+k$  of  $\pi$  form a, say, south-east chain, the same is true for the entries in columns  $i, i+1, \dots, i+k-1$



of  $j(\pi)$ , since this is the case if and only if the sequence of partitions along the top border of the restricted filling is  $\emptyset, 1, 11, 111, \dots$ .

Similarly, if the entries in rows  $i, i+1, \dots, i+k-1$  form, for example, a north-east chain, the same is true for the entries in the same rows of  $j(\pi)$ , since this is the case if and only if the sequence of partitions along the right border of the restricted filling is  $\emptyset, 1, 2, 3, \dots$ .

In Section 6 we will also need the following proposition, for which, unfortunately, we do not have a short proof:

**Proposition 4.5.** *Consider the following two growth diagrams:*

$$\begin{array}{|c|c|c|} \hline \nu & \lambda & \tau \\ \hline \end{array} \quad \text{and} \quad \begin{array}{|c|c|c|} \hline \nu & \mu & \tau \\ \hline \end{array},$$

*and suppose furthermore that  $\lambda$  and  $\mu$  are Knuth equivalent and of the same size. Then, applying  $j$  to both diagrams we obtain*

$$\begin{array}{|c|c|c|} \hline \nu' & \lambda' & \tau' \\ \hline \end{array} \quad \text{and} \quad \begin{array}{|c|c|c|} \hline \nu' & \mu' & \tau' \\ \hline \end{array},$$

*where  $\nu'$  has exactly one column less than  $\nu$  and  $\tau'$  has exactly one more column than  $\tau$ . In this situation,  $\lambda'$  and  $\mu'$  are Knuth equivalent.*

*Similarly, consider*

$$\begin{array}{|c|} \hline \tau \\ \hline \lambda \\ \hline \nu \\ \hline \end{array} \quad \text{and} \quad \begin{array}{|c|} \hline \tau \\ \hline \mu \\ \hline \nu \\ \hline \end{array},$$

*and suppose furthermore that  $\lambda$  and  $\mu$  are dual Knuth equivalent. Then, applying  $j$  to both diagrams we obtain*

$$\begin{array}{|c|} \hline \tau' \\ \hline \lambda' \\ \hline \nu' \\ \hline \end{array} \quad \text{and} \quad \begin{array}{|c|} \hline \tau' \\ \hline \mu' \\ \hline \nu' \\ \hline \end{array},$$

*where  $\nu'$ ,  $\lambda'$  and  $\tau'$  have as many rows as  $\nu$ ,  $\lambda$  and  $\tau$  respectively. In this situation,  $\lambda'$  and  $\mu'$  are dual Knuth equivalent.*

*Proof.* The proof is given in Appendix A. □

To apply the transformation  $j$  to a rectangular diagram with an arbitrary filling  $\pi$ , we first separate the entries using one of the methods described in Section 3.3. Then we apply the transformation  $j$  to the new diagram as many times as there are entries in the first column of  $\pi$  counting multiplicities. Finally we shrink the diagram back again, such that column  $i$  of the transformed diagram contains as many entries, counting multiplicities, as column  $i+1$  of the original diagram, and the last column of the transformed diagram contains as many entries, counting multiplicities, as the first column of the original diagram.

Note that, due to Corollary 4.4 the final step is well defined. For example, if we use Burge's method to separate the entries, in each set of columns that yields a single column in the shrunk diagram, the entries form a south-east chain. The same is true for each set of rows that yields a single row in the shrunk diagram.

Intuitively, we are pushing the entries in the first column towards the end. Note that, unfortunately, in general the transformation  $j$  does not preserve the number of entries of a given size, if we are using one of the first two methods of Section 3.3 to separate the entries of the diagram. For example, using Burge's method,  $\begin{array}{|c|c|} \hline 1 & 1 \\ \hline 1 & 1 \\ \hline \end{array}$  is

mapped to  $\begin{array}{|c|c|} \hline 2 & \\ \hline & 1 \\ \hline \end{array}$ . However, there is a notable exception to this failure: 0-1-fillings

where each non-zero entry is the only one in its row or column are mapped to 0-1-fillings with the same restriction. Of course, if we use the method corresponding to RSK' or dual RSK, this is also the case.

## 5. INCREASING AND DECREASING SUBSEQUENCES IN FILLINGS OF MOON POLYOMINOES

In this section we will apply the transformation  $j$  defined in Definition 4.1 to moon polyominoes, thus proving a conjecture of Jakob Jonsson [9, 10].

**Definition 5.1.** The *content* of a moon polyomino is the sequence of column heights, in decreasing order.

For example, the content of the moon polyomino at the left of Figure 1 is  $(7, 6, 5, 4, 3, 3, 2)$ , while the content of the other two polyominoes in the same figure is  $(5, 4, 4, 3, 2, 2, 2)$ .

**Theorem 5.2.** *Consider 0-1-fillings of a given moon polyomino with exactly  $m_i$  non-zero entries in row  $i$ , such that the length of the longest north-east chain equals  $k$ . Then the number of these fillings does not depend on the order of the columns, given that the resulting polyomino is again a moon polyomino. Furthermore, if we disregard the number of entries in row  $i$ , the number of fillings depends only on the content of the moon polyomino.*

Special cases of this theorem were proved by Jakob Jonsson and Volkmar Welker [9, 10] and by Christian Krattenthaler [12]. More precisely, in [10] the special case of stack polyominoes is proved, using a very different method. In [12] the special case of Ferrers shapes is dealt with. For the connection between [12] and our method, see Section 7.

We prove this theorem in two steps. First we show that the transformation  $j$  from Definition 4.1 can be used to prove an analogous result about arbitrary fillings. In a second step we show that this implies the theorem above, albeit in a non-bijective fashion. Thus, the problem of finding a completely bijective proof of Theorem 5.2 remains open. However, it appears that this problem is difficult: only very recently, Sergi Elizalde [7] solved the first non-trivial case, which is  $k = 2$ , but only for Ferrers diagrams.

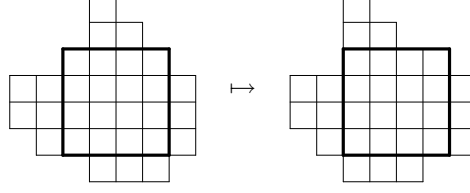
**Proposition 5.3.** *Consider arbitrary fillings of a given moon polyomino, where the sum of the entries in row  $i$  equals  $m_i$ , the length of the longest ne-chain equals  $k$  and the length of the longest SE-chain equals  $l$ .*

*Then the number of these fillings does not depend on the order of the columns, given that the resulting polyomino is again a moon polyomino. Furthermore, if we disregard the number of entries in row  $i$ , the number of fillings depends only on the content of the moon polyomino.*

*Similarly, we can fix the length of the longest NE- and the longest se-chain. If we restrict ourselves to 0-1-fillings, we can fix the length of the longest nE- and the longest Se-chain, or, alternatively, the length of the longest Ne- and the longest sE-chain.*

*Proof.* We first show that reordering the columns of the moon polyomino such that the result is again a moon polyomino does not change the number of fillings in question. It suffices to show this in the following special case: let  $c$  be any column of the moon polyomino that is contained in one of the columns to its right. Consider the largest rectangle completely contained in the moon polyomino that has the same height as  $c$ . Then moving the first column of this rectangle to its

end does not change the number of fillings. For example, we could modify a moon polyomino as follows:



We now apply the following bijective transformation to the filling of the moon polyomino: all the entries outside of the rectangle stay as they are, whereas we apply the transformation  $j$  to the entries within the rectangle.

Obviously, the sum of the entries in each row remains the same. Furthermore, due to Corollary 4.4, this transformation preserves the length of the longest chains.

To prove the second claim, we first sort the columns according to their height, using the transformation just described, in decreasing order. This is possible, because moon polyominoes are intersection-free.

Suppose now that we want to preserve the length of nE- and Se-chains. We then reflect the polyomino about the line  $x = y$ , to obtain a stack polyomino. Note that this reflection transforms nE- into Ne-chains and Se- into sE-chains.

Now we sort the columns of the resulting stack polyomino according to height, preserving the maximum lengths of Ne- and sE-chains, and obtain a Ferrers shape.

Reflecting this shape again about the line  $x = y$  we obtain a Ferrers shape with the same content as the original moon polyomino, such that both the length of the longest nE-chain and the length of the longest Se-chain are preserved.

The other three cases are dealt with similarly.  $\square$

Unfortunately, the proof above does not work for Theorem 5.2. As we have observed before, the transformation  $j$  does not preserve the number of entries of a given size. However, we can use simple facts about simplicial complexes and the Stanley-Reisner ring to prove the result.

*Proof of Theorem 5.2.* Consider the simplicial complex  $\Delta$  of 0-1 fillings of the moon polyomino, having at most  $m_i$  non-zero entries in row  $i$  and whose length of the longest north-east chain is at most  $k$ .

The Stanley-Reisner ring of  $\Delta$  is the polynomial ring having variables  $x_{ij}$  for each square  $(i, j)$  in the moon polyomino, modulo the relations

$$(2) \quad \{x_{i_0 j_0} x_{i_2 j_2} \dots x_{i_k j_k} = 0 : (i_0 j_0), (i_2 j_2), \dots, (i_k j_k) \text{ is a north-east chain in } \Delta\}.$$

Thus, there is an obvious bijection between monomials in this ring and arbitrary fillings of the moon polyomino satisfying the restrictions of the theorem.

Similarly, we can consider the simplicial complex  $\Delta'$  of 0-1 fillings of the transformed moon polyomino, having at most  $m_i$  non-zero entries in row  $i$  and whose length of the longest north-east chain is at most  $k$ .

Lemma 5.3 tells us that the number of monomials of given degree in the Stanley-Reisner ring corresponding to  $\Delta$  is the same as the number of monomials of the same degree in the Stanley-Reisner ring corresponding to  $\Delta'$ . That is, the Hilbert functions of the two rings must be the same. Thus the corresponding simplicial complexes must have the same  $f$ -vector, which is equivalent to the claim of the theorem.  $\square$

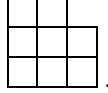
*Remark.* Note that in Theorem 5.2 we cannot restrict the length of the longest SE-chain instead, not even for stack polyominoes. Although the set of 0-1-fillings whose longest SE-chain has length at most  $l$  is still a simplicial complex, there is no longer a bijection between the monomials of the associated Stanley-Reisner ring

and arbitrary fillings of the moon polyomino satisfying the appropriate restrictions. The reason is that the relations in (2) do not exclude chains containing multiple entries.

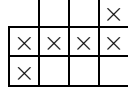
Indeed, consider the following filling of a stack polyomino:



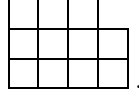
Its longest SE-chain has length 3. However, there is no such filling with seven non-zero entries of the stack polyomino



Similarly, we cannot preserve simultaneously the length of the longest ne- and se-chain, at least not if we insist on preserving the number of entries in each row. For example,



is a filling with longest north-east chain having length two, and longest south-east chain having length one. On the other hand, there is no such filling of the polyomino



As we hinted at before, it would be interesting to have a completely bijective proof of Theorem 5.2. We believe that this may well be accomplished using a modification of the Backelin-West-Xin-transformation introduced in [3]. Note that results similar to ours were obtained by Anna de Mier [6] using this transformation. For additional information, see [4, 12].

## 6. A COMMUTATION PROPERTY

In this section we would like to prove another beautiful feature of the transformation  $j$  as applied in the proof of Lemma 5.3:

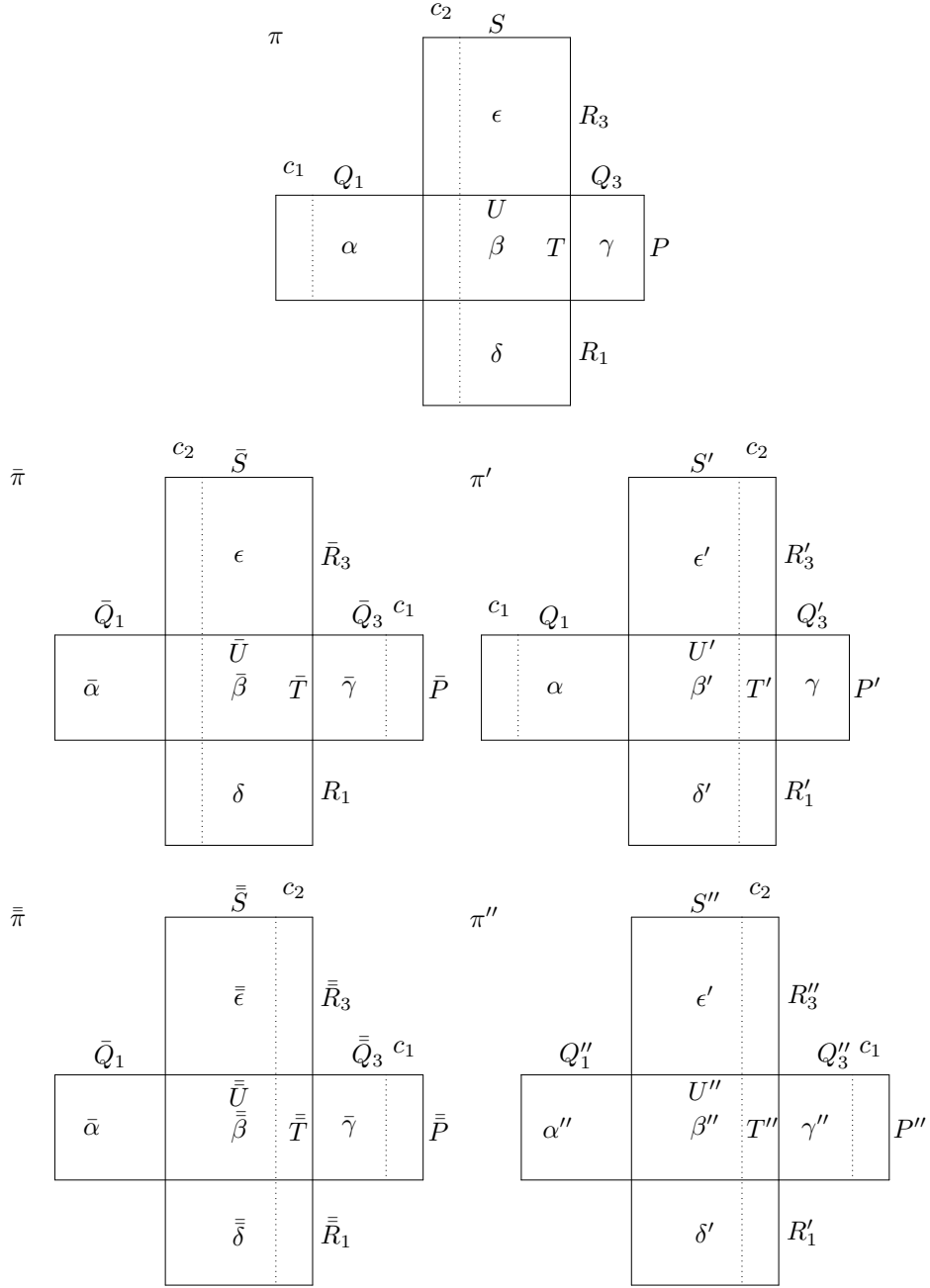
**Proposition 6.1.** *Applications of  $j$  to different maximal rectangles of a moon-polyomino commute with each other.*

*Proof.* Suppose that  $c_1$  and  $c_2$  are respectively the first columns of two maximal rectangles  $\Gamma$  and  $\Delta$  and that we want to move  $c_1$  to the end of the first rectangle, and  $c_2$  towards the end of the second rectangle. Since all entries outside of these two rectangles stay unchanged, we can assume that the moon polyomino consists only of the union of  $\Gamma$  and  $\Delta$ , as schematically depicted at the top of Figure 7. There, we subdivided  $\Gamma$  into three smaller rectangles  $\alpha$ ,  $\beta$  and  $\gamma$  and  $\Delta$  into  $\delta$ ,  $\beta$  and  $\epsilon$ .

In the following we will have to consider several growth diagrams simultaneously. We denote the sequences of partitions labelling the corners along the top and right borders of  $\Gamma = \begin{bmatrix} \alpha & \beta & \gamma \end{bmatrix}$  with  $(Q_1, Q_2, Q_3)$  and  $P$  respectively. The sequences of

partitions labelling the top and right borders of  $\Delta = \begin{bmatrix} \epsilon \\ \beta \\ \delta \end{bmatrix}$  will be  $S$  and  $(R_1, R_2, R_3)$ .

Furthermore, we consider the growth diagram corresponding to  $\beta$  and will label its top and right border with sequences of partitions  $U$  and  $T$ .


 FIGURE 7. Applying  $j$  successively to  $\Gamma$  and  $\Delta$ 

On the left hand side of Figure 7 we see what happens to the original filling when we apply  $j$  first to the rectangle  $\Gamma = \begin{bmatrix} \alpha & \beta & \gamma \end{bmatrix}$ , to obtain  $\bar{\pi}$ , and then to  $\begin{bmatrix} \epsilon \\ \beta \\ \delta \end{bmatrix}$  to obtain  $\bar{\bar{\pi}}$ . On the right hand side the result  $\pi'$  of applying  $j$  first to the rectangle

$\Delta = \begin{bmatrix} \epsilon \\ \beta \\ \delta \end{bmatrix}$  and then the result  $\pi''$  of applying  $j$  to  $\boxed{\alpha} \boxed{\beta'} \boxed{\gamma}$  is shown. We have to

prove that the fillings  $\bar{\pi}$  and  $\pi''$  at the bottom of Figure 7 are the same.

We first observe that  $\boxed{\beta}$  and  $\boxed{\beta'}$  are Knuth equivalent. This follows by applying

the second part of Corollary 4.4 to the rows corresponding to  $\beta$  in  $\begin{bmatrix} \epsilon \\ \beta \\ \delta \end{bmatrix}$ . Thus we can

apply the first part of Proposition 4.5 with  $\nu = \alpha$ ,  $\lambda = \beta$ ,  $\mu = \beta'$  and  $\tau = \gamma$  and obtain that  $\bar{\alpha} = \alpha''$ ,  $\bar{\gamma} = \gamma''$  and  $\bar{T} = T''$ . Again by the second part of Corollary 4.4,

applied to the rows corresponding to  $\bar{\beta}$  in  $\begin{bmatrix} \epsilon \\ \bar{\beta} \\ \delta \end{bmatrix}$  we have that  $\bar{T} = \bar{\bar{T}}$ .

Very similarly, applying the first part of Corollary 4.4, we observe that  $\boxed{\beta}$  and  $\boxed{\bar{\beta}}$  are dual Knuth equivalent. Thus, the second part of Proposition 4.5 with  $\nu = \delta$ ,  $\lambda = \beta$ ,  $\mu = \bar{\beta}$  and  $\tau = \epsilon$  shows that  $\bar{\delta} = \delta'$ ,  $\bar{\epsilon} = \epsilon'$  and  $\bar{U} = U'$ . By the first part of Corollary 4.4 we have  $U' = U''$ .

Finally,  $\bar{\beta} = \beta''$  follows from  $\bar{T} = T''$  and  $\bar{U} = U''$ .  $\square$

## 7. EVACUATION AND JEU DE TAQUIN FOR STACK POLYOMINOES

In this section we relate our bijection to evacuation, and thereby to the construction employed by Christian Krattenthaler [12] to prove Theorem 5.2 and 5.3 for the special case of Ferrers diagrams. We refer the reader to Christian Krattenthaler's article for more on this subject.

Let us first recall the definition of evacuation. Given a weakly increasing sequence of partitions  $P = (\emptyset = \lambda^0, \lambda^1, \dots, \lambda^n)$ , we construct the *evacuated* sequence of partition  $ev(P) = (\emptyset = \mu^0, \mu^1, \dots, \mu^n)$  as follows: We set  $\mu^n = \lambda^n$ , and then  $\mu^{n-i}$  equal to the last partition of  $jdt(\dots jdt(P))$ , where we apply  $jdt$   $i$  times.

Regarding evacuation, we recall the following two important facts:

**Fact 7.1** (Theorem A 1.2.10 and Corollary A 1.2.11 of [15]). *If  $\pi$  corresponds to  $(P, Q)$  then the filling obtained from  $\pi$  by rotation about  $180^\circ$  corresponds to  $(ev(P), ev(Q))$ .*

*If  $\pi$  corresponds to  $(P, Q)$  then the filling obtained by reversing the order of the columns of  $\pi$  corresponds to  $(P^t, ev(Q)^t)$ .*

Christian Krattenthaler [12] used the following bijection on Ferrers shapes:

**Definition 7.2.** Let  $\pi$  be a filling of a Ferrers shape and  $\Delta$  the associated growth diagram. Let  $e(\Delta)$  be the growth diagram obtained from  $\Delta$  by transposing all the partitions along the top and right border and applying the backward rules B1 to B4 to obtain the remaining partitions and the entries of the squares. Let  $e(\pi)$  be the filling associated to  $e(\Delta)$ .

In this section we show that the growth-diagram bijections used by Christian Krattenthaler are to evacuation what our transformation  $j$  is to *jeu de taquin*. To this end we extend the notion of growth diagrams introduced in Section 3 to stack polyominoes. For brevity, we will describe our construction in terms of Greene's Theorem 3.2.

We label the corners of a stack polyomino with two partitions each:

- an *upper partition*, which is given by applying Greene's Theorem to the rectangular region below and to the left of the corner, as wide as the row just above the corner and

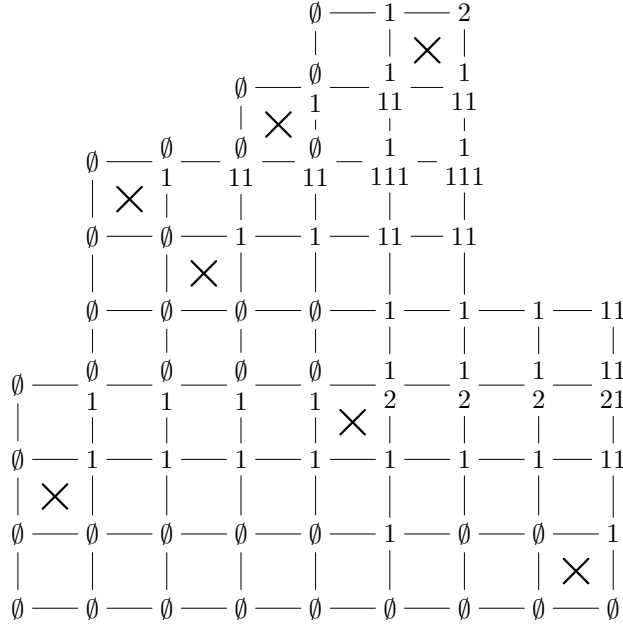


FIGURE 8. a growth diagram for a stack polyomino

- a *lower partition*, which is given by applying Greene's Theorem to the rectangular region below and to the left of the corner, as wide as the row just below the corner.

Of course, if the rows just below and just above the corner are left justified, the two partitions are the same. In this case we will only indicate one partition. In particular, for Ferrers shapes the construction above coincides with the obvious extension of growth diagrams as presented in Section 3 and introduced by Sergey Fomin and Tom Roby [8, 14]. An example of such a generalised growth diagram is given in Figure 8.

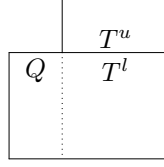
Similar to the growth diagrams for rectangular shapes we have the following proposition:

**Proposition 7.3.** *The sequences of partitions along the borders of a generalised growth diagram determine its entries.*

*Proof.* Suppose we have reconstructed the growth diagram up to its  $i^{\text{th}}$  row, counted from the top, including the sequence of upper partitions along the bottom of this row. If the following row starts at the same column, lower and upper partitions coincide and we proceed using the usual backward rules B1 to B4 as given in Section 3 to obtain the entries of the row and the sequence of upper partitions labelling its bottom corners. Otherwise, it is necessary to reconstruct the sequence of lower partitions labelling the bottom of the  $i^{\text{th}}$  row first. As the following fact shows, this can be done.  $\square$

**Fact 7.4.** *In the situation of Figure 9,  $T^l$  is determined by  $T^u$  and the final partition in  $Q$ .*

*Proof.* Observe that by Proposition 4.2  $T^u$  can be obtained from  $(Q, T^l)$  by applying  $jdt$  as many times as there are partitions in  $Q$ . It is easy to see using growth diagrams that this implies the uniqueness of  $T^l$ .  $\square$

FIGURE 9. reconstructing  $T^l$  from  $Q$  and  $T^u$ 

It remains to state precisely in which way we apply *jeu de taquin* to a given filling. The bijection we will relate to  $e$  is defined as follows:

**Definition 7.5.** Let  $\pi$  be a filling of a Ferrers shape  $F$ . Apply  $j^{-1}$  to move the second column to the first position, then the third column to the first position and so on, to obtain the filling  $j^*(\pi)$ .

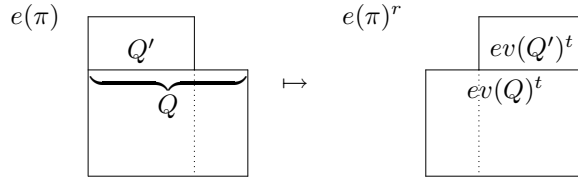
Finally, we can state and prove the main theorem of this section:

**Theorem 7.6.** Let  $\pi$  be a filling of a Ferrers shape  $F$ . Let  $e(\pi)^r$  be the filling obtained by reflecting  $e(\pi)$  about a vertical line. Then  $j^*(\pi) = e(\pi)^r$ .

*Proof.* We first recall that the statement is well known for rectangular shapes  $F$ : let the sequence of partitions labelling the right corners of  $\pi$  be  $P$  and let  $Q$  be the sequence of partitions labelling the top corners. Then, by Proposition 4.2, applying  $j^*$  to  $\pi$  amounts to applying evacuation on  $Q$  and leaving  $P$  unchanged.

Finally, by Fact 7.1, reversing the order of the columns of  $j^*(\pi)$  amounts to applying evacuation on both  $P$  and  $ev(Q)$  and transposing the resulting tableaux. Thus, in this case  $\pi^r$  corresponds to tableaux  $P^t$  and  $ev(ev(Q))^t = Q^t$ , which are by definition the tableaux corresponding to  $e(\pi)$ .

To prove the general case, we use the notion of generalised growth diagrams and show that the partitions labelling the corners along the borders of  $j^*(\pi)$  are the same as those of  $e(\pi)^r$ .

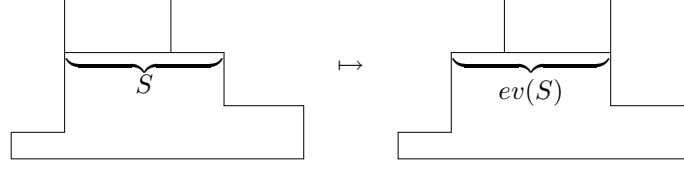
FIGURE 10. corresponding rows of  $e(\pi)$  and  $e(\pi)^r$ 

We first describe the partitions labelling the corners of  $e(\pi)^r$ . Let  $Q_i$  be the sequence of partitions just above the  $i^{\text{th}}$  row of  $e(\pi)$ . Let  $S_i^u$  be the sequence of upper partitions just above the  $i^{\text{th}}$  row of  $e(\pi)^r$  and  $S_i^l$  the sequence of lower partitions. Then,  $S_i^l = ev(Q_i)^t$ . Furthermore, if, counting from the top, the  $i^{\text{th}}$  and  $(i-1)^{\text{st}}$  row of  $e(\pi)$  have the same length,  $S_i^u = S_i^l = ev(Q_i)^t$ . Otherwise, let  $Q'_i$  be the sequence of partitions consisting of the first  $l$  elements of  $Q_i$ , where  $l$  is the length of the  $(i-1)^{\text{st}}$  row. We then have  $S_i^u = ev(Q'_i)^t$ .

In Figure 10 the correspondence just described is shown schematically. For the proof, we only need to appeal to Fact 7.1.

We now turn to the partitions on the left border of  $j^*(\pi)$ . Consider the effect of moving a block of columns of the same height to the left, as sketched in Figure 11. We remark that subsequent moves of necessarily smaller columns from the right




 FIGURE 11. applying  $j^{-1}$  to a block of columns

to the left do not affect the partitions labelling the corners along the border of columns already moved.

Thus, suppose that the corners along the top border of the largest rectangle containing the last column are labelled with a sequence of partitions  $S$  and suppose that the last  $l$  columns of  $\pi$  are of the same height. By definition, the first  $l$  lower partitions in  $j^*(\pi)$  in the same row are just the first  $l$  elements of  $ev(S)$ . Taking into account what we have shown before, this coincides with the labelling obtained by reversing  $e(\pi)$ .

It is easy to see that the partitions labelling the right border of  $e(\pi)^r$  and  $j^*(\pi)$  coincide as well.  $\square$

#### APPENDIX A. THE TRANSFORMATION $j$ PRESERVES KNUTH EQUIVALENCE IN SUB-RECTANGLES

In this appendix we prove Proposition 4.5.

**Definition A.1.** Two growth diagrams differ by a *Knuth relation of the first kind*, if all but three columns coincide, and the remaining three columns are related (schematically) by transforming

$$\begin{array}{|c|c|c|} \hline & \times & \\ \times & & \times \\ \hline & \times & \\ \hline \end{array} \text{ into } \begin{array}{|c|c|c|} \hline & & \times \\ \times & \times & \\ \hline & \times & \\ \hline \end{array},$$

or vice versa. They differ by a *Knuth relation of the second kind*, if the remaining three columns are related by transforming

$$\begin{array}{|c|c|} \hline \times & \\ \times & \times \\ \hline \times & \\ \hline \end{array} \text{ into } \begin{array}{|c|c|} \hline \times & \\ \times & \times \\ \hline \times & \\ \hline \end{array},$$

or vice versa.

The indicated transformations are called *Knuth transformations*.

It is well known that two growth diagrams are Knuth equivalent if and only if they can be transformed one into the other using a sequence of Knuth transformations. The following proposition gives also some information on the sequence of partitions along the upper border of the growth diagram. For its precise statement, we need yet another definition:

**Definition A.2.** A partial filling of a rectangle with three columns is *shape equivalent to a triangle*, if the partition labelling the top right corner of the corresponding growth diagram equals 21.

**Proposition A.3.** Two fillings differ by a single Knuth relation (of either kind), namely in columns  $k-1$ ,  $k$  and  $k+1$  if and only if the fillings are Knuth equivalent, the sequences of partitions along the top border of their growth diagrams differ in exactly one partition, namely either between columns  $k-1$  and  $k$  or  $k$  and  $k+1$ , and the fillings restricted to these three columns are shape equivalent to a triangle.

Note that there are Knuth equivalent growth diagrams that differ in exactly one partition along the top border, but cannot be transformed one into the other by a single Knuth transformation. A small example is given in Figure 12, where we superimposed the two growth diagrams, using crosses for one and circles for the other. Furthermore, we write partitions belonging to the diagram with circles just above the partitions belonging to the diagram with crosses, wherever the partitions labelling a corner differ. We will keep this notation throughout the appendix.

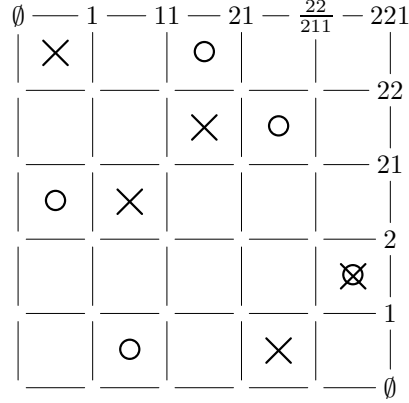


FIGURE 12. Two very different fillings, whose growth diagrams differ along the border only in a single partition.

*Proof.*  $\ominus$  If two fillings differ by a single Knuth relation, then the sequences of partitions along the top border of their growth diagrams differ in exactly one partition.

Suppose that the two growth diagrams differ by a single Knuth relation of the first kind, as shown in Figure 13.a. In this case, all partitions along the top border up to and including the partition just after column  $k-1$  must be equal, since, up to this point the fillings are identical. Furthermore, all partitions along the top corner starting with the partition just after column  $k+1$  must be equal, since the fillings up to that column are Knuth equivalent, and thereafter identical. We conclude that, in this case, exactly the partitions of the two growth diagrams on the top border just after column  $k$  are different.

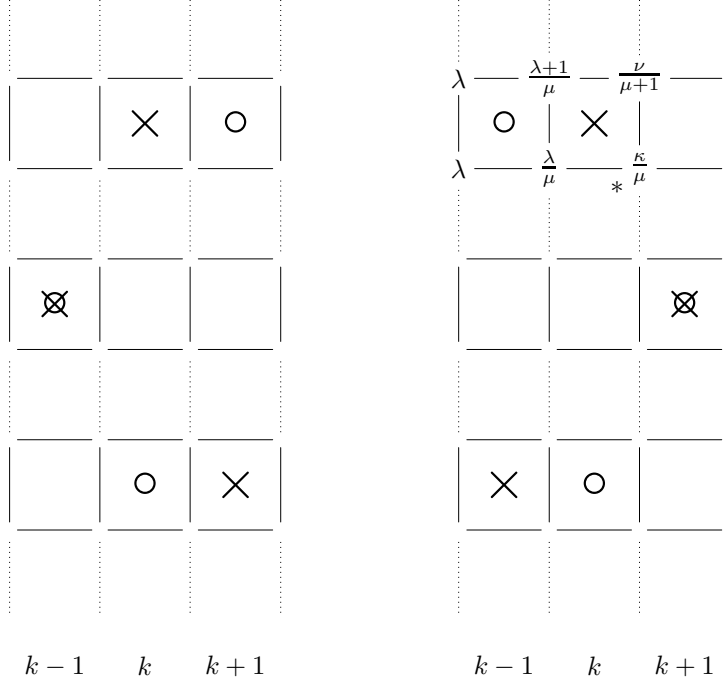
It remains to check the case where the two growth diagrams differ by a single Knuth relation of the second kind.

To ease the description, we introduce the following notation: given a partition  $\lambda$ , let  $\lambda + \epsilon_k$  be the result of adding one to the  $k^{\text{th}}$  part of  $\lambda$ . Furthermore, we write  $\lambda + 1$  as shorthand for  $\lambda + \epsilon_1$ . We then have a situation as shown schematically in Figure 13.b.

We first show that, in the situation of Figure 13.b, either  $\mu = \lambda + 1$  or  $\nu = \mu + 1$ . To this end, suppose that  $\mu \neq \lambda + 1$ . Since the fillings in the rectangles below and to the left of  $*$  are equal, with the exception of the position of an empty column,  $\mu = \kappa$ . Applying forward rule F2, it follows that  $\nu = \mu \cup \lambda + 1 = \mu + 1$ .

It remains to show that the two growth diagrams differ in exactly one of the two partitions on the top border. If  $\mu = \lambda + 1$ , then all partitions on the right side above the circle in column  $k-1$  are identical, by the forward rules, including the partition on the top border.

If, however,  $\nu = \mu + 1$ , we have to use an inductive argument to show our claim. Consider the following part of a growth diagram, where both boxes are assumed to be empty and  $r \neq s$ :



a. Knuth relation of the first kind.    b. Knuth relation of the second kind.

FIGURE 13. Knuth equivalent columns

$$\begin{array}{ccccc}
 \kappa & \text{-----} & & \text{-----} & \\
 | & & & | & \\
 \lambda & \text{-----} & \frac{\lambda + \epsilon_r}{\lambda + \epsilon_s} & \text{-----} & \lambda + \epsilon_r + \epsilon_s
 \end{array}$$

We will show that no matter what value  $\kappa$  has, there will be again exactly one corner at the top where the partitions of the two growth diagrams differ:

Suppose first, that  $\kappa = \lambda + \epsilon_r$  and  $s = r + 1$ . Applying the forward rules F2 and F3 we obtain

$$\begin{array}{ccccc}
 \kappa = \lambda + \epsilon_r & \text{-----} & \lambda + \epsilon_r + \epsilon_{r+1} & \text{-----} & \\
 | & & & | & \\
 \lambda & \text{-----} & \frac{\lambda + \epsilon_r}{\lambda + \epsilon_{r+1}} & \text{-----} & \lambda + \epsilon_r + \epsilon_{r+1}
 \end{array}$$

Thus the partitions labelling corners on the right of the first column of the two growth diagrams coincide from hereon, and the claim follows.

If  $\kappa = \lambda + \epsilon_r$ , but  $r \neq s$ , we obtain

$$\begin{array}{ccccc}
 \kappa = \lambda + \epsilon_r & \text{-----} & \frac{\lambda + \epsilon_r + \epsilon_{r+1}}{\lambda + \epsilon_r + \epsilon_s} & \text{-----} & \lambda + \epsilon_r + \epsilon_{r+1} + \epsilon_s \\
 | & & & | & \\
 \lambda & \text{-----} & \frac{\lambda + \epsilon_r}{\lambda + \epsilon_s} & \text{-----} & \lambda + \epsilon_r + \epsilon_s
 \end{array}$$

Finally, if  $\kappa = \lambda + \epsilon_t$ , with all of  $r$ ,  $s$  and  $t$  being different, we obtain

$$\begin{array}{ccccc} \kappa = \lambda + \epsilon_t & \text{---} & \frac{\lambda + \epsilon_r + \epsilon_t}{\lambda + \epsilon_s + \epsilon_t} & \text{---} & \lambda + \epsilon_r + \epsilon_s + \epsilon_t \\ | & & | & & | \\ \lambda & \text{---} & \frac{\lambda + \epsilon_r}{\lambda + \epsilon_s} & \text{---} & \lambda + \epsilon_r + \epsilon_s \end{array}$$

In both cases, the situation in the corners of the top row is the same as in the bottom row, and the claim follows.

⊕ If the sequences of partitions along the top border of two Knuth equivalent growth diagrams differ in exactly one partition, namely between columns  $k$  and  $k+1$ , and the three columns  $k-1$ ,  $k$  and  $k+1$  or  $k$ ,  $k+1$  and  $k+2$  are shape equivalent to a triangle, then the corresponding fillings differ by a single Knuth relation in these three columns.

Distinguishing between several cases, we consider the effect of applying the backward rules B1 to B4 to the partitions labelling the corners of columns  $k-1$ ,  $k$  and  $k+1$ . We will show that, in each row, if not all partitions coincide, either the partitions between columns  $k$  and  $k+1$  or those between column  $k-1$  and  $k$  differ, and all others coincide. Working our way from the top of the growth diagrams to their bottom, we can distinguish three stages: in Stage 1, the partitions between columns  $k$  and  $k+1$  differ. This stage can be followed either by Stage 2 or by Stage 3. In Stage 2, the partitions between columns  $k-1$  and  $k$  differ and only Stage 3 can follow. Finally, Stage 3 correspond to those rows, that lie between the entries which are swapped by the Knuth transformation. It is followed by those rows in which all partitions coincide.

Throughout the rest of this proof we will maintain  $r < s$ . To make it easier to keep track of the various situations and make the description more concise, we omit cases which may be obtained by exchanging the two growth diagrams. The backward rules we apply are printed into the corresponding cells wherever appropriate.

- (1) During this stage, the partitions of the two growth diagrams between columns  $k$  and  $k+1$  differ. The Cases c and f lead directly to Stage 3, whereas Case e leads to Stage 2. All other cases stay within Stage 1.

$$\begin{array}{ccccc} \lambda - \epsilon_r - \epsilon_s & \text{---} & \frac{\lambda - \epsilon_r}{\lambda - \epsilon_s} & \text{---} & \lambda \\ | & & | & & | \\ \kappa & \text{---} & & \text{---} & \kappa \end{array}$$

- (a)  $\kappa = \lambda - \epsilon_t$  and  $r$ ,  $s$  and  $t$  are all different.

$$\begin{array}{ccccc} \lambda - \epsilon_r - \epsilon_s & \text{---} & \frac{\lambda - \epsilon_r}{\lambda - \epsilon_s} & \text{---} & \lambda \\ | & \text{B2} & | & \text{B2} & | \\ \kappa - \epsilon_{r-1} - \epsilon_s & \text{---} & \frac{\kappa - \epsilon_r}{\kappa - \epsilon_s} & \text{---} & \kappa = \lambda - \epsilon_t \end{array}$$

- (b)  $\kappa = \lambda - \epsilon_r$  and  $r > 1$ .

$$\begin{array}{ccccc} \lambda - \epsilon_r - \epsilon_s & \text{---} & \frac{\lambda - \epsilon_r}{\lambda - \epsilon_s} & \text{---} & \lambda \\ | & \frac{\text{B2}}{\text{B1}} & | & \frac{\text{B3}}{\text{B2}} & | \\ \kappa - \epsilon_{r-1} - \epsilon_s & \text{---} & \frac{\kappa - \epsilon_{r-1}}{\kappa - \epsilon_s} & \text{---} & \kappa = \lambda - \epsilon_r \end{array}$$

(c)  $\kappa = \lambda - \epsilon_r$  and  $r = 1$ .

$$\begin{array}{ccccc}
 \lambda - \epsilon_1 - \epsilon_s & \xrightarrow{\quad \frac{\lambda - \epsilon_1}{\lambda - \epsilon_s} \quad} & \lambda & & \\
 \downarrow & \text{B2} & \downarrow & \text{B4} & \downarrow \\
 \kappa - \epsilon_s & \xrightarrow{\quad \frac{\kappa}{\kappa - \epsilon_s} \quad} & \kappa = \lambda - \epsilon_1 & & \\
 \times & & \circ & & 
 \end{array}$$

(d)  $\kappa = \lambda - \epsilon_s$  and  $r \neq s - 1$ .

$$\begin{array}{ccccc}
 \lambda - \epsilon_r - \epsilon_s & \xrightarrow{\quad \frac{\lambda - \epsilon_r}{\lambda - \epsilon_s} \quad} & \lambda & & \\
 \downarrow & \text{B3} & \downarrow & \text{B2} & \downarrow \\
 \kappa - \epsilon_r - \epsilon_{s-1} & \xrightarrow{\quad \frac{\kappa - \epsilon_r}{\kappa - \epsilon_{s-1}} \quad} & \kappa = \lambda - \epsilon_s & & \\
 & & & & 
 \end{array}$$

Note that, since  $r < s$ , we have automatically  $s > 1$ .

(e)  $\kappa = \lambda - \epsilon_s$  and  $r = s - 1 > 1$ .

In this case we also have to consider the partitions labelling corners of columns  $k - 1$  and  $k + 2$ .

$$\begin{array}{ccccccc}
 \lambda - \epsilon_{s-1} - \epsilon_s - \epsilon_t & \cdot & \lambda - \epsilon_{s-1} - \epsilon_s & \xrightarrow{\quad \frac{\lambda - \epsilon_{s-1}}{\lambda - \epsilon_s} \quad} & \lambda & \xrightarrow{\quad} & \lambda + \epsilon_u \\
 \downarrow & & \downarrow & \text{B3} & \downarrow & \text{B2} & \downarrow \\
 \mu & \xrightarrow{\quad \frac{\kappa - 2\epsilon_{s-1}}{\kappa - \epsilon_{s-2} - \epsilon_{s-1}} \quad} & \kappa - \epsilon_{s-1} & \xrightarrow{\quad} & \kappa = \lambda - \epsilon_s & \xrightarrow{\quad} & 
 \end{array}$$

It turns out that in this case columns  $k$ ,  $k + 1$  and  $k + 2$  cannot be shape equivalent to a triangle. We first observe that this would force  $u = s$ : if  $u < s$ , columns  $k$ ,  $k + 1$  and  $k + 2$  would form a row in the diagram corresponding to circles, if  $u > s$ , columns  $k$ ,  $k + 1$  and  $k + 2$  would form a column in the diagram corresponding to crosses.

However, if  $u = s$ , we have a cell

$$\begin{array}{ccc}
 \lambda & \xrightarrow{\quad} & \lambda + \epsilon_s \\
 \downarrow & & \downarrow \\
 \lambda - \epsilon_s & \xrightarrow{\quad} & 
 \end{array}$$

which is impossible, considering the local rules.

We conclude that columns  $k - 1$ ,  $k$  and  $k + 1$  must be shape equivalent to a triangle. By reasoning similar to above we find  $t = s - 1$  and therefore  $\mu = \kappa - \epsilon_{s-2} - 2\epsilon_{s-1}$  by B3 and B2 respectively.

(f)  $\kappa = \lambda - \epsilon_s$  and  $r = s - 1 = 1$ .

This case is very similar to the preceding one, the only difference being that the cell in column  $k - 1$  will now contain a circle, the cell in column  $k$  a cross.

(2) Within this stage, the partitions between columns  $k - 1$  and  $k$  of the two growth diagrams differ. We show that cases in this stage can only be followed by cases of Stage 2 or 3.

$$\begin{array}{ccccccc}
 \lambda - \epsilon_r - \epsilon_s & \xrightarrow{\quad \frac{\lambda - \epsilon_r}{\lambda - \epsilon_s} \quad} & \lambda & \xrightarrow{\quad} & \lambda + \epsilon_t & & \\
 \downarrow & & \downarrow & & \downarrow & & \\
 \kappa - \epsilon_u - \epsilon_v & \xrightarrow{\quad \frac{\kappa - \epsilon_u}{\kappa - \epsilon_v} \quad} & \kappa & \xrightarrow{\quad} & \kappa + \epsilon_w & & 
 \end{array}$$

This situation occurs after Case 1e and thus can only occur if columns  $k$ ,  $k+1$  and  $k+2$  are not shape equivalent to a triangle. Throughout this subcase, in the situation of the diagram above, we maintain  $r < t \leq s$ . Note that this condition is satisfied by the partitions along the bottom of the diagram in Case 1e. We are going to show that we also have  $u < w \leq v$  or that we are in one of the cases of Stage 3.

- (a)  $\kappa = \lambda - \epsilon_x$  and  $r, s$  and  $x$  are all different.

By B2 we obtain  $\kappa - \epsilon_u = \lambda - \epsilon_r \cap \lambda - \epsilon_x$  and thus  $u = r$ . Similarly, we have  $v = s$ . To determine  $w$ , we consider the cell

$$\begin{array}{ccc} \lambda & \text{-----} & \lambda + \epsilon_t \\ | & & | \\ \lambda - \epsilon_x & \text{-----} & \lambda - \epsilon_x + \epsilon_w \end{array}$$

If  $w = x$ , we obtain  $w = t - 1$ . Since  $r \neq x = w$  and  $r \leq t - 1 = w$  we also have  $u = r < w = t - 1 \leq v = s$ .

If, however,  $w \neq x$ , then we have by the local rules in fact  $w = t$ .

- (b)  $\kappa = \lambda - \epsilon_s$ .

By B2 we obtain  $u = r$ , by B3 that  $v = s - 1$ . Now consider

$$\begin{array}{ccc} \lambda & \text{-----} & \lambda + \epsilon_t \\ | & & | \\ \lambda - \epsilon_s & \text{-----} & \lambda - \epsilon_s + \epsilon_w \end{array}$$

If  $w = s$ , the local rules imply  $t = s + 1$ , which contradicts our assumption  $t \leq s$ . Thus,  $w \neq s$ , which entails  $w = t$ . Since  $t = s$  is impossible by the local rules, we have indeed  $u = r < w = t \leq v = s - 1$ .

- (c)  $\kappa = \lambda - \epsilon_r$  and  $r > 1$ .

By B3 we obtain  $u = r - 1$  and by B2  $v = s$ . To determine  $w$ , we consider the cell

$$\begin{array}{ccc} \lambda & \text{-----} & \lambda + \epsilon_t \\ | & & | \\ \lambda - \epsilon_r & \text{-----} & \lambda - \epsilon_r + \epsilon_w \end{array}$$

If  $w = r$  we immediately have  $u = r - 1 < w = r \leq v = s$ . If  $w \neq x$ , we obtain  $w = t$  and  $u = r - 1 < w = t \leq v = s$ .

- (d)  $\kappa = \lambda - \epsilon_r$  and  $r = 1$ .

In this case the growth diagram looks as follows:

$$\begin{array}{ccccc} \lambda - \epsilon_1 - \epsilon_s & \text{-----} & \frac{\lambda - \epsilon_1}{\lambda - \epsilon_s} & \text{-----} & \lambda & \text{-----} & \lambda + \epsilon_t \\ | & \times & | & \circ & | & & | \\ \lambda - \epsilon_1 - \epsilon_s & \text{-----} & \frac{\lambda - \epsilon_1}{\lambda - \epsilon_1 - \epsilon_s} & \text{-----} & \kappa = \lambda - \epsilon_1 & \text{-----} & \lambda - \epsilon_1 \end{array}$$

$\frac{\text{B2}}{\text{B4}} \quad \quad \quad \frac{\text{B4}}{\text{B2}}$

We are thus lead to a situation of Stage 3.

- (3) In this final stage, the growth diagram is of one of the following forms:

(a)  $u \neq s$

$$\begin{array}{ccccc} \lambda - \epsilon_r & \text{---} & \frac{\lambda}{\lambda - \epsilon_r} & \text{---} & \lambda \\ | & & | & & | \\ \lambda - \epsilon_u - \epsilon_r & \text{---} & \frac{\lambda - \epsilon_u}{\lambda - \epsilon_u - \epsilon_r} & \text{---} & \lambda - \epsilon_u \end{array}$$

(b)  $r > 1$

$$\begin{array}{ccccc} \lambda - \epsilon_r & \text{---} & \frac{\lambda}{\lambda - \epsilon_r} & \text{---} & \lambda \\ | & & | & & | \\ \lambda - \epsilon_{r-1} - \epsilon_r & \text{---} & \frac{\lambda - \epsilon_r}{\lambda - \epsilon_{r-1} - \epsilon_r} & \text{---} & \lambda - \epsilon_r \end{array}$$

(c)

$$\begin{array}{ccccc} \lambda - \epsilon_1 & \text{---} & \frac{\lambda}{\lambda - \epsilon_1} & \text{---} & \lambda \\ | & & | & & | \\ \lambda - \epsilon_1 & \text{---} & \lambda - \epsilon_1 & \text{---} & \lambda - \epsilon_1 \end{array}$$

$\bigcirc$ 
 $\times$

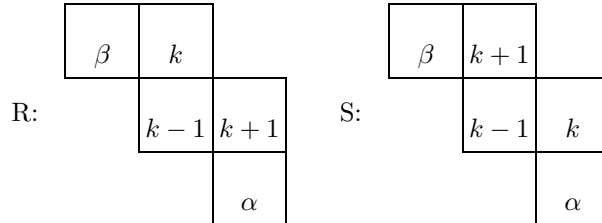
By considering the different cases as detailed above, the reader will easily convince herself of the validity of the claim.  $\square$

**Lemma A.4.** *Let  $R$  be a partial Young tableau and construct another partial Young tableau  $S$  by exchanging the entries  $k$  and  $k+1$  in  $R$ . Suppose that the entries  $k-1$ ,  $k$  and  $k+1$  of both  $R$  and  $S$  are shape equivalent to a triangle. Then  $\overline{jdt}(S)$  can be obtained from  $\overline{jdt}(R)$  by exchanging entries  $k-1$  and  $k$ .*

*Similarly, suppose that  $S$  was obtained from  $R$  by exchanging the entries  $k-1$  and  $k$ , and entries  $k-1$ ,  $k$  and  $k+1$  of both  $R$  and  $S$  are shape equivalent to a triangle. Then  $\overline{jdt}(S)$  can be obtained from  $\overline{jdt}(R)$  by either exchanging entries  $k-2$  and  $k-1$  or entries  $k-1$  and  $k$ .*

*Proof.* Consider the effect of applying the algorithm  $jdt$  as introduced in the beginning of Section 4 to  $R$ . If the two boxes whose entries differ in  $R$  and  $S$  are not adjacent, their entries will never be compared by the algorithm, and the statement follows trivially. Otherwise, consider the case that entries  $k$  and  $k+1$  were swapped to obtain  $S$  from  $R$ .

Since entries  $k-1$ ,  $k$  and  $k+1$  are shape equivalent to a triangle in both  $R$  and  $S$ , and the boxes containing  $k$ ,  $k+1$  are supposed to be adjacent, the boxes containing  $k-1$ ,  $k$  and  $k+1$  must be arranged as follows:

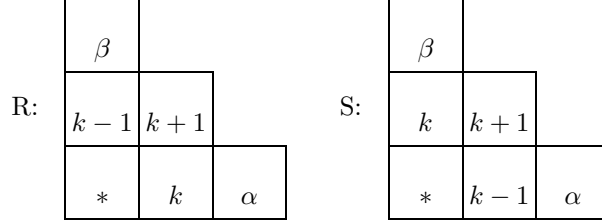


If  $k-1$  were in a higher row, the entries  $k-1$ ,  $k$  and  $k+1$  would form a single row in  $R$ , if  $k-1$  were in a lower row, they would form a column in  $S$ .

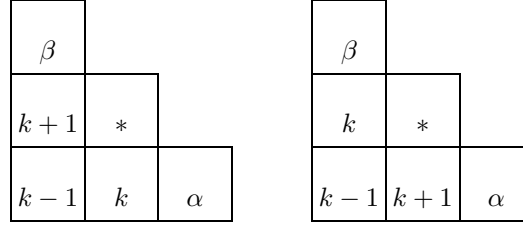
However, we now observe that both  $\alpha$  and  $\beta$  must be smaller than  $k-1$ , since entries in rows and columns are strictly increasing. Thus, in this case,  $jdt$  can never swap the empty box with the box containing  $k-1$ . Taking into account that  $jdt$

subtracts one from all entries, we conclude that  $jdt(S)$  can be obtained from  $jdt(R)$  by exchanging entries  $k - 1$  and  $k$ .

We now consider the case that entries  $k - 1$  and  $k$  were swapped to obtain  $S$  from  $R$  and the boxes containing  $k - 1$  and  $k$  are adjacent. Then, the boxes containing  $k - 1$ ,  $k$  and  $k + 1$  must be arranged as follows:



In this situation, both  $\alpha$  and  $\beta$  must be greater than  $k + 1$ . Thus, if during  $jdt$  the empty box is moved to the place marked with a  $*$  above, after two steps of the algorithm we have the following situations:



Thus, only entries  $k$  and  $k + 1$  are exchanged. Taking into account that  $jdt$  subtracts one from all entries, we conclude that  $jdt(S)$  can be obtained from  $jdt(R)$  by exchanging entries  $k - 1$  and  $k$ .

If  $jdt$  does not happen to compare entries  $k - 1$  and  $k$ ,  $jdt(S)$  can be obtained from  $jdt(R)$  by exchanging entries  $k - 2$  and  $k - 1$ .

Since  $\bar{jdt}$  and  $jdt$  differ only by the box containing the largest entry, the claim follows.  $\square$

*Proof of Proposition 4.5.* To prove the first statement, we observe that  $\lambda$  and  $\mu$  can be transformed one into the other using a sequence of Knuth transformations. Thus, we only need to consider the case where  $\lambda$  and  $\mu$  differ by a single Knuth relation. In this situation, Proposition A.3 and Lemma A.4 apply, and the claim follows.

The second statement follows by similar reasoning directly from Proposition A.3. We only have to observe that the notions of Knuth equivalence and dual Knuth equivalence are connected by reflecting diagrams about the main diagonal.  $\square$

## REFERENCES

- [1] Christos A. Athanasiadis, *On noncrossing and nonnesting partitions for classical reflection groups*, Electronic Journal of Combinatorics **5** (1998), Research Paper 42, 16 pp. (electronic).
- [2] Christos A. Athanasiadis and Victor Reiner, *Noncrossing partitions for the group  $D_n$* , SIAM Journal on Discrete Mathematics **18** (2004), no. 2, 397–417 (electronic).
- [3] Jürgen Backelin, Julian West, and Guoce Xin, *Wilf-equivalence for singleton classes*, Advances in Applied Mathematics (to appear).
- [4] Mireille Bousquet-Melou and Einar Steingrímsson, *Decreasing subsequences in permutations and Wilf equivalence for involutions*, Journal of Algebraic Combinatorics (2005), no. 4, 383–409, math.CO/0405334.
- [5] William Y. C. Chen, Eva Y. P. Deng, Rosena R. X. Du, Richard P. Stanley, and Catherine H. Yan, *Crossings and nestings of matchings and partitions*, Transactions of the American Mathematical Society (2006), math.CO/0501230.
- [6] Anna de Mier,  *$k$ -noncrossing and  $k$ -nonnesting graphs and fillings of Ferrers diagrams*, math.CO/0602195.



- [7] Sergi Elizalde, *A bijection between 2-triangulations and pairs of non-crossing Dyck paths*, Preprint (2006), math.CO/0610235.
- [8] Sergey Fomin, *The generalized Robinson-Schensted-Knuth correspondence*, Zapiski Nauchnykh Seminarov Leningradskogo Otdeleniya Matematicheskogo Instituta imeni V. A. Steklova Akademii Nauk SSSR (LOMI) **155** (1986), no. Differentsialnaya Geometriya, Gruppy Li i Mekh. VIII, 156–175, 195.
- [9] Jakob Jonsson, *Generalized triangulations and diagonal-free subsets of stack polyominoes*, Journal of Combinatorial Theory, Series A **112** (2005), no. 1, 117–142.
- [10] Jakob Jonsson and Volkmar Welker, *A Spherical Initial Ideal for Pfaffians*, (2006), math.CO/0601335.
- [11] Anisse Kasraoui and Jiang Zeng, *Distribution of crossings, nestings and alignments of two edges in matchings and partitions*, math.CO/0601081.
- [12] Christian Krattenthaler, *Growth diagrams, and increasing and decreasing chains in fillings of Ferrers shapes*, Advances in Applied Mathematics **37** (2006), 404–431, math.CO/0510676.
- [13] Victor Reiner, *Non-crossing partitions for classical reflection groups*, Discrete Mathematics **177** (1997), no. 1-3, 195–222.
- [14] Tom Roby, *Applications and extensions of Fomin’s generalization of the Robinson-Schensted correspondence to differential posets*, Ph.D. thesis, M.I.T., Cambridge, Massachusetts, 1991.
- [15] Richard P. Stanley, *Enumerative combinatorics*, vol. 2, Cambridge University Press, 1999.